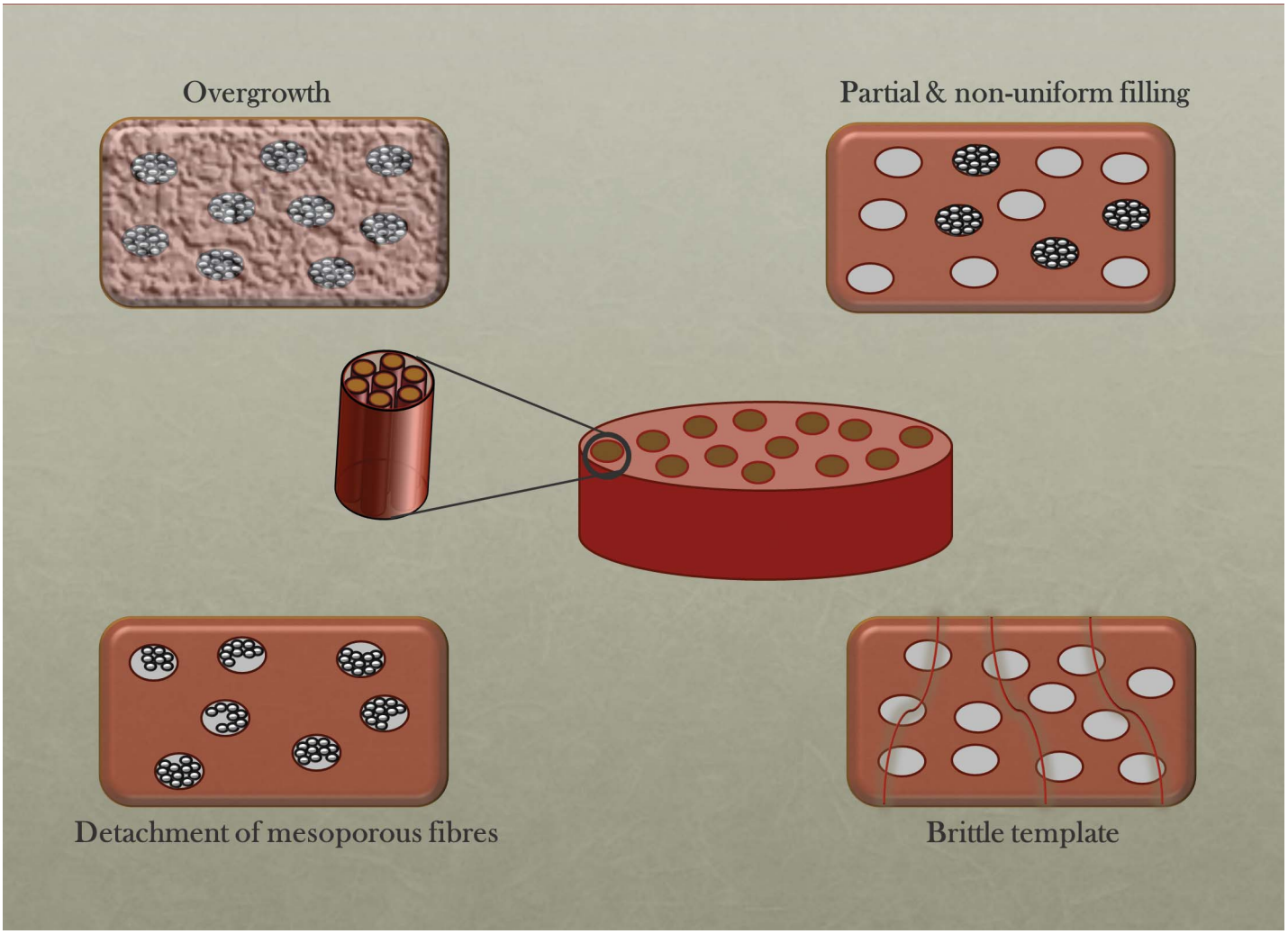

Showing the work of hierarchically structured membranes presented by S. Meoto, Department of Chemical Engineering, University College London. Part of this work was carried out at Rensselaer Polytechnic Institute, U.S.A.

Title: Anodic alumina-templated synthesis of mesostructured silica membranes – Current status and challenges

Synthesis of mesoporous silica/anodic alumina membranes has been extensively researched. Our findings are summarized, comparing various techniques and also significant challenges that will greatly affect the essential membrane application.

As featured in:

See S. Meoto and M.-O. Coppens, *J. Mater. Chem. A*, 2014, **2**, 5640.

ROYAL SOCIETY OF CHEMISTRY

www.rsc.org/MaterialsA

Registered charity number: 207890

Journal of Materials Chemistry A

PAPER

Cite this: J. Mater. Chem. A, 2014, 2, 5640

Anodic alumina-templated synthesis of mesostructured silica membranes – current status and challenges

Silo Meoto and Marc-Olivier Coppens*

Received 20th December 2013
Accepted 27th February 2014

DOI: 10.1039/c3ta15330d

www.rsc.org/MaterialsA

Numerous fabrication methods have been employed in the preparation of anodic alumina-confined, ordered mesoporous silica membranes. The sol–gel and aspiration techniques appear to be the most promising, but realizing a completely filled, crack free, hybrid membrane is still a challenge on macroscopic scales. Presented in this paper are current synthetic challenges involved in the formation of such a hierarchically structured membrane. Overcoming these challenges is essential to use these hybrid materials for membrane separations.

1. Introduction

Since its discovery, ordered mesoporous silica has attracted much attention because of its unique properties, such as a very narrow pore size distribution, highly ordered pores of uniform and adjustable size, a high specific surface area, and a high pore volume.[1–3] While early investigations were mostly focused on particulates,[4–8] recent studies have increasingly focused on the synthesis of thin films[9,10] and a variety of other morphologies.[11–13] Mesoporous silica is synthesized by a self-assembly process conducted in an aqueous precursor solution containing a surfactant as structure-directing agent (SDA).[14] A critical step in the process is the formation of a periodic structure in which micelles of the SDA are surrounded by polycondensing silica, *via* a cooperative self-assembly process.[15–17] The polymerization of the mesoporous silica is carried out by an acid (or base)-catalyzed hydrolysis and condensation reaction, generally described by the following three steps:[18,19]

$$\equiv Si-OR + H_2O \overset{\text{hydrolysis}}{\rightleftharpoons} \equiv Si-OH + ROH \quad (1)$$

$$\equiv Si-OR + HO-Si\equiv \overset{\text{alcohol condensation}}{\rightleftharpoons} \equiv Si-O-Si + ROH \quad (2)$$

$$\equiv Si-OH + HO-Si\equiv \overset{\text{water condensation}}{\rightleftharpoons} \equiv Si-O-Si\equiv + H_2O \quad (3)$$

When ordered mesoporous silica is synthesized, the mesostructure tends to orient itself parallel to the solid–liquid interface, *e.g.*, in films or grown on a solid support.[10,20,21] To have more control over the orientation and textural features of the synthesized silica, self-assembly of tuneable silica mesostructures was carried out within the confining channels of a porous substrate. Martin[22,23] first reported the synthesis of nanomaterials within the channels of a porous membrane, which acts as a "hard" template. Among these hard templates, porous alumina membranes are a popular choice because their well-ordered structure is mechanically and chemically stable, and they have parallel pores that are oriented perpendicularly to the external membrane surface. Manufactured electrochemically, their pore size ranges from tens to hundreds of nanometres.[24] As a result, they can be used for the fabrication of solid nanomaterials with controlled diameter and aspect ratio.[25] Numerous studies have reported the use of a porous anodic alumina membrane (AAM) to fabricate hierarchically structured silica materials. Channels of AAM have been used to form silica nanowires,[26] nanofibres[27,28] and nanotubes.[29] Synthesis of a hybrid material for membrane applications is, however, what concerns us mostly in this paper. As the pores of the silica materials are so much narrower and vertically aligned, a hybrid composite membrane consisting of mesoporous silica confined within anodic alumina channels makes a promising candidate for size-exclusive separation of molecules. This hybrid membrane forms the ideal 'pores within pores' molecular filter system proposed by Martin[30] wherein the silica nanochannels, acting as a molecular sieve, can be tailored to reliably separate small molecules on the basis of their size, increasing the selectivity, as well as, by a proper pore surface chemistry, the permeability of the membrane.

To synthesize mesostructured silica within the channels of AAM, a silica precursor sol solution is introduced into the AAM pores, which can be done in several ways. Using the sol–gel method, Mitchell *et al.*[31] prepared silica nanotubes and attached hydrophilic and hydrophobic functional groups on their inner surface (while inside the alumina template) and

Department of Chemical Engineering, University College London, Torrington Place, London, WC1E 7JE, UK. E-mail: m.coppens@ucl.ac.uk; Fax: +44 (0)20 7383 2348; Tel: +44 (0)20 7679 7369

outer surface (after removing the alumina template). They collected the formed silica nanotubes from the alumina matrix and used these differently functionalized nanotubes to extract lipophilic molecules from an aqueous solution. In 2003, Yang *et al.*[29] prepared 1D mesostructured silica nanotubes and nanofibres in porous AAM by a sol–gel induced solvent evaporation process. After five minutes, AAM modified with octachlorosilane had become transparent, suggesting that its pores were completely filled. However, the membrane was immersed in the precursor solution for 12 h to ensure complete infiltration. By using a hydrophobically modified AAM, they were able to reduce the process time from days to hours. Lu *et al.*[32] also used the sol–gel method proposed by Zhao and co-workers[4] to grow SBA-15 nanorod arrays in alumina membranes. In their procedure, the porous AAM was immersed in the precursor solution at room temperature for 20 h. The gelation period lasted for another 20 h, at 60 °C. The long aging time was used to ensure the formation of a rigid silica network with a highly ordered mesostructure. In 2005, Jin *et al.*[26] obtained highly ordered 1D mesoporous silica within alumina membranes by adjusting the aging process and water content. Their procedure included a rotary evaporator to enhance evaporation of the volatile component. Following this step, the hybrid membrane was aged for 12 h at 60 °C. They found that the arrangement and orientation of the synthesized silica nanowires were sensitive to the aging conditions during the formation procedure. In the presence of water, the rate of solvent evaporation is slow, giving enough time for nucleation and growth, so that the silica nanowires can replicate the shape of the AAM pores. Tube-like silica nanowires were obtained after the dissolution of the AAM. Ku *et al.*[33] proposed a multi-stage approach to solve the problem of incomplete filling of AAM pore channels. Their procedure involved repeated immersion of the membrane template after calcination, to allow additional deposits of the precursor solution. They carried out a gas permeability measurement, which showed a significant drop in the permeability of the synthesized MS–AAM composite membrane compared to the empty (control) AAM.

Taking a different track and using the EISA method, a group led by Bein[44,48] has focused on studying the formation mechanism, structure and orientation of mesoporous silica confined in AAM. They showed that, when ionic surfactant CTAB is used, columnar silica with hexagonally ordered mesopores is obtained, in which the pores are oriented along the AAM channels. However, with non-ionic surfactants P123 and Brij 56, circular or columnar or a mixture of both orientations can be obtained, depending on the silica-to-surfactant ratio and the humidity level. An increase in surfactant concentration at high humidity shifts the mesostructure from the circular to columnar orientation. Their results also showed that a lower concentration of surfactant in the deposition solution leads to a less ordered structure and an associated decrease in the intensity of the diffraction spots seen in the small-angle X-ray scattering (SAXS) patterns. However, TEM images revealed that about 30% of the alumina matrix was not filled with silica. Subsequent work by Platschek *et al.*[47] introduced an inorganic salt to the deposition mixture to help form a phase-pure columnar mesoporous silica when non-ionic surfactants are used. An additional benefit observed with this salt-induced method is less shrinkage of the silica from the AAM pore walls after calcination. It was suggested that adding inorganic salt increases the chemical interactions between the silica and the alumina wall. It was also demonstrated that the transformation from circular to columnar phases for Brij 56 occurs at temperatures above 30 °C. Another group led by Frey[52,54] has used the same method to fabricate mesostructured silica within the channels of AAM using a tetrahydrofuran-based solution. In their most recent report,[54] the surface of the AAM channels was modified to control the orientation of the in-channel mesostructures. They proposed that a more negatively charged AAM surface decreased the amount of protons available in the solution inside the channels, which leads to slower silica condensation. Delaying silica condensation allows for longer transformation times and results in higher abundance and larger domains of the columnar phase. The results also showed good contact between the hexagonal mesostructures and the alumina channel walls, with good filling in each alumina channel.

In 2004, Yamaguchi and co-workers[55] proposed a new method to synthesize mesostructured silica inside AAM channels. Using moderate aspiration, they formed silica with CTAB-templated mesopores inside AAM channels. These silica mesopores were estimated to be about 3.4 nm in diameter. The size-exclusion separation capability of the as-synthesized composite membrane was demonstrated using molecules of different molecular sizes: molecules larger than the channel diameter were rejected. In 2008 they used the same method with silica templated by different surfactants, P123 and F127. Varying the temperature and aging time during the sol preparation, they reported 1D aligned mesostructures for P123 at 30 °C and 60 °C and long aging times (>7 h). On the other hand, a short aging time (2 h) and low temperature (0 °C) resulted in 3D mesostructures. For F127, only columnar silica with non-parallel mesopores was obtained, regardless of the synthesis conditions.[59] The 1D nanochannels formed using P123 were found to always be 8 ± 2 nm in diameter, which is much bigger than the nanochannels formed using CTAB in their previous study. The F127-induced channel diameter was estimated to be *ca.* 12 nm. Other groups have also employed the aspiration method to synthesize the MS–AAM nanosystem, like El-Safty *et al.*,[62,63,66] who developed a simple method to fabricate silica cylinders inside AAM channels by coating both the AAM and the inner surface of the formed silica mesostructures with organic moieties to make them chemically robust. Prior to the infiltration of the precursor solution, the pore channels of AAM were modified with *N*-trimethoxysilylpropyl-*N*,*N*,*N*-trimethylammonium chloride (TMAC). This led to the formation of tight silica mesocylinders without air gaps.[61] The fabricated hybrid membranes, containing silica nanotubes with a pore diameter $\leq$ 4 nm, were used as a filter to separate noble metal nanoparticles, semiconductor nanocrystals of varying sizes, and cytochrome C (CytC) into homogeneous groups and sizes within seconds. They were also used for the rapid separation of biomolecules such as insulin, α-amylase, β-lactoglobulin and myosin proteins.

Table 1 Overview of reported procedures for the synthesis of MS–AAM composite membranes[a]

Reference	SDA	Molar ratio SiO_2 : SDA : EtOH : H^+ : H_2O	Precursor solution (aging) time; temp.	(Membrane) synthesis (aging) time; temp. [other parameters]	Morphology	Application
Sol–gel						
13	—	1 : 0 : 17 : 0.04 : 4	2–30 days; RT, 2–15 days; 50 °C	1 day; RT (1 min dipped)	Nanofibres of hollow and solid cores, tubules if aging > 23 days, diameters of 30 nm and length 6 μm	/
34	—	1 : 0 : 17 : 0.02 : 4	2, 5, 10, 15, 25, 30 days; 20 °C	2, 5, 10, 15, 25, 30 days; 20 °C (1 min dipped)	Nanowires (2,5,10 & 15 days of aging time) Nanotubes (25 & 30 days of aging time)	/
31	—	—	—	—	Nanotubes	Nanophase extractors; silica nanotubes used to remove lipophilic molecules from aqueous solution
29	F127	1 : 0.01 : 3.3 : 0.56 : 0	2 h; RT	2 h in air, 1 h at 60 °C (12 h contact)	Circular structured nanofibres and nanotubes	/
35	P123	1 : 0.02 : 11 : 0.55 : 0	10 min; 37 °C	25 min; 40 °C	Aged out of sol → tubular structures Aged in sol → denser rod/wire-like structures Increased water content → highly ordered hexagonally arranged mesoporous silica	/
25	P123	—	—	—	Nanowires with S-helices and D-helices	/
36	P123	1 : 0.01 : 9 : 0.001 : 6 1 : 0.03 : 24 : 0.003 : 17	3 h	24 h; 25 °C (12 cm min^{-1} dipping speed)	2D hexagonal cylindrical mesostructure Lamella structure	/
32	P123	1 : 0.02 : 11 : 0.55 : 0	10 min; RT	20 h; 25 °C, 20 h; 60 °C	Uniform nanorods; hexagonally arranged	/
33	CTAC	/	10 min; RT	1–2 days; RT	P123, CTAC → concentric and hexagonal channels	/
	P123	/			F127 → pores packed in a cubic arrangement	
	F127	1 : 0.05 : 92 : 5.3 : 111				
26	P123	1 : 0.02 : 11 : 0.54 : 0	10 min; 37 °C	25 min; 40 °C	Aged at 60 °C, 12 h → tube-like shell and hexagonally arranged silica nanowire Water added to aging sol → circular nanochannels formed	/
11	P123	1 : 0.02 : 32 : 0.27 : 11	2 h; RT	2 h (5, 15, & 20 h); 100 °C	1D mesoporous tubes formed 2 h → nanotubes with a height of 0.5 μm 5 h, 15 h, 20 h → length of 1–10 μm	/
37	Brij 56	1 : 0.1 : 9 : 3 : 0	30 min; RT	15 min; RT, 15 min; 45 °C	Cubic mesostructure	Gas permeation
38	F127	1 : 0.01 : 11 : 4.5 : 0	5 min; RT	1–2 days; RT	Mesoporous pores ~13–16 nm in diameter	Air permeability measurements
28	P123	1 : 0.02 : 153 : 2.5	20 min; RT	—; RT	P123 < 0.15 mg mL^{-1} → nanochannels aligned along the axis of MSNF	/
		1 : 0.06 : 153 : 2.5		12 h; 60 °C	P123 < 0.3 mg mL^{-1} → circular lamellar mesostructure	
39	CTAB	1 : 0.14 : 3.5 : 0.02 : 8	2 h; RT	5 h; RT		/

Table 1 (*Contd.*)

Reference	SDA	Molar ratio SiO_2 : SDA : EtOH : H^+ : H_2O	Precursor solution (aging) time; temp.	(Membrane) synthesis (aging) time; temp. [other parameters]	Morphology	Application
					Columnar mesochannels inside the AAO pores, continuous silica film over the AAO template	
40	—	1 : 0 : 38.9 : 0.05 : 0	12 h	20 min	Nanotubes of uniform structure and ultra-thin wall thickness	Affinity experiments and adsorption of bilirubin
41	F127	1 : 0.01 : 5 : 0.01	—	48 h; RT, 24 h; 70 °C	Nanofibres with a structural mixture of helices with straight core nanochannels and multilayer stacked helix nanochannels	Fabrication of gold nanofibres
42	P123	1 : 0.02 : 9 : 0.7	3 h; 35 °C	4 days; RT, 24 h; 90 °C	Mesostructured silica, with hybrid membrane porosity of 0.1	/
1	P123	1 : 0.02 : 147 : 2.4	2 h; RT	24 h; RT	Mesostructured nanofibres	Fabrication of cobalt nanorods
43	P123	— : 5×10^{-4} : 0 : 0.007 : 0.44	1 h; 38 °C	—	2 mL P123 added → mesoporous structures perforating the wall of the silica nanotubes	/
		— : 3×10^{-4} : 0 : 0.007 : 0.44			1 mL P123 added → mesochannels circling the axis of the silica nanotube	
		— : 3×10^{-3} : 0 : 0.007 : 0.44			0.5 mL P123 added → mixture of perpendicular, circling and/or parallel alignment of mesopores	
EISA						
44	CTAB	1 : 0.2 : 26 : 8 : 10 1 : 0.3 : 26 : 8 : 10	1 h; 60 °C	3–5 h; RT (0.75 mL dropped)	CTAB → hexagonally structured mesopores	/
	Brij 56	1 : 0.01 : 34 : 8 : 10 1 : 0.02 : 34 : 8 : 10			P123, Brij 56 → circular and columnar mesopore orientation	
	P123	1 : 0.13 : 60 : 8 : 10 1 : 0.3 : 60 : 8 : 10			Increase in surfactant concentration → shifts population towards the columnar mesostructures	
45	P123	1 : 0.01 : 33 : 0.05 : 10	1 h; 60 °C	2 h; RT (0.75 mL dropped)	Circular to columnar orientation by adding inorganic salts	/
46	P123	1 : 0.01 : 34 : 8 : 10 1 : 0.02 : 43 : 8 : 10	1 h; 60 °C	26 °C (0.75 mL dropped)	Low surfactant concentration → hexagonal phases with circular or columnar orientation	/
	Brij 56	1 : 0.13 : 34 : 8 : 10 1 : 0.3 : 60 : 8 : 10	5 min; RT		High surfactant concentration → additional tubular lamellar structure	

Table 1 (*Contd.*)

Reference	SDA	Molar ratio SiO_2 : SDA : EtOH : H^+ : H_2O	Precursor solution (aging) time; temp.	(Membrane) synthesis (aging) time; temp. [other parameters]	Morphology	Application
47	P123	1 : 0.01 : 34 : 0.05 : 10	1 h; 60 °C	21 °C, 30 °C (1 mL dropped)	Addition of salt → stable columnar mesostructures	/
	Brij 56	1 : 0.13 : 34 : 0.05 : 10	5 min; RT			
48	CTAB	1 : 0.3 : 33 : 8 : 10	1 h; 60 °C	26 °C (0.75 mL dropped)	CTAB → columnar hexagonal structures form directly from the beginning	/
	Brij 56	1 : 0.3 : 76 : 8 : 10			P123 → circular hexagonal structures form first and directly transform into columnar hexagonal phase after complete evaporation of the solvent	
	P123	1 : 0.01 : 44 : 8 : 10			Brij 56 → circular hexagonal structures form first and directly transform into a mixture or columnar and tubular lamellar phase after complete evaporation of the solvent	
49	CTAB	1 : 4:9 : 8 : 10	1 h; 60 °C	3–5 h; RT (0.75 mL dropped)	Columnar mesostructure → drug loading dependent on pore diameter. Increase in pore diameter increases release rate	Drug uptake and release experiments
	P123 (circ.)	1 : 0.003 : 9:8 : 10			Circular mesostructure → limited pore access prevents significant adsorption of drug. Drug is promptly released, although only approx. 70%	
	P123/ NaCl (col.)	1 : 0.003 : 9:8 : 10				
50	CTAB	1 : 1.8 : 33 : 0.2 : 110	1 h; 60 °C	(0.75 mL dropped)	CTAB → hexagonal circular mesophase	/
	Brij 56	1 : 0.3 : 33 : 0.2 : 110			P123 → cubic *Imm* phase	
51	P123	1 : 0.01 : 35 : 0.06 : 3	1 h; 60 °C	Overnight; 27 °C (0.75 mL dropped)	Hexagonal columnar mesophase (induced by the addition of lithium chloride salt)	Deposition of Cu and Ag
52	P123	1 : 0.02 : 14* : 3 1 : 0.02 : 14* : 3	1 h	RT (0.05 mL dropped)	High humidity (90%) → ordered undistorted, circular & columnar hexagonal phase mesostructures	/
	Brij 56	1 : 0.14 : 14* : 3 1 : 0.17 : 14* : 3			Low humidity → circular lamellar phase, but distorted structures	
53	P123	1 : 0.01 : 35 : 8 : 10	1 h; 60 °C	30 °C (2 drops)	Hexagonal columnar mesophase (induced by the addition of lithium chloride salt)	Albumin zero-order release experiments
54	P123	1 : 0.02 : 14* : 3	1 h	(0.05 mL) RT	Mesostructures with dominant circular hexagonal phase and occasional columnar hexagonal phase Circular to columnar phase transformation enhanced in highly negatively charged surfaces	/

Table 1 (*Contd.*)

Reference	SDA	Molar ratio SiO_2 : SDA : EtOH : H^+ : H_2O	Precursor solution (aging) time; temp.	(Membrane) synthesis (aging) time; temp. [other parameters]	Morphology	Application
Aspiration						
55	CTAB	1 : 0.1 : 9 : 0.6 : 0	90 min; 60 °C	RT	Columnar mesoporous structures *ca.* 20 μm in length	Molecular transport
56	CTAB	1 : 0.1 : 9 : 0.004 : 0	90 min; 60 °C 30 min	RT	—	Capture and release of solutes by permeation of phenol, benzene sulfonate and benzene disulfonate
57	CTAB	1 : 0.1 : 9 : 0.004 : 0	90 min; 60 °C 30 min	RT	—	Extraction of charged organic dye molecules
58	CTAB	1 : 0.1 : 9 : 0.004 : 0	90 min; 60 °C 30 min	RT	Columnar structures ~50 μm in length	Diffusivity measurements of tris(2,2′-bipyridyl)-ruthenium
59	P123 F127	1 : 0.02 : 32 : 0.3 : 11 1 : 0.01 : 40 : 0.6 : 8	2–24 h; 0, 30, 60 °C	RT (4 mL dropped) (5 min drying)	Channel diameter of silica nanochannel 8 ± 2 nm. Optimal conditions 1D alignment nanochannels → (P123) 60 °C, 12 h 3D alignment nanochannels → (P123) 0 °C, 2 h F127 → only columnar mesostructures with non-parallel orientation and channel diameter of 12 nm & only suitable for the synthesis of 3D hybrid MS	/
60	F127	1 : 0.01 : 40 : 0.6 : 8	1 h; 30 °C 5 h; 30 °C	RT	Reagent concentration < 15 mM → columnar mesostructured silica Reagent concentration > 20 mM → disordered needle-like silica structures	/
61	CTAB DDAB	1 : 0.2 : 8 : 2 1 : 0.2 : 8 : 2	30 min; RT	10 h; 45 °C; 0.04 MPa	Hexagonal nanotubes	Filtration of nanoparticles, nanocrystals and cytochrome c
62	CTAB Brij 98 P123	1 : 0.2 : 17 : 3 1 : 0.1 : 17 : 3 1 : 0.01 : 17 : 3	—	10 h; 45 °C; 0.04 MPa	Hexagonal 2D mesocylinder	Filtration to separate high concentration macromolecules *e.g.* lysozyme, cytochrome c, myoglobin, β-lactoglobulin, haemoglobin
63	F127	1 : 0.01 : 17 : 3	—	10 h; 45 °C; 0.04 MPa	Addition of dodecane → formation of 3D cubic *Im3m* structures	Separation of lysozyme, myoglobin, β-lactoglobulin, haemoglobin

Table 1 (*Contd.*)

Reference	SDA	Molar ratio SiO_2 : SDA : EtOH : H^+ : H_2O	Precursor solution (aging) time; temp.	(Membrane) synthesis (aging) time; temp. [other parameters]	Morphology	Application
64	Brij-type	1 : 0.08 : 9 : 1.5	2.5 h; 30 °C	—	2D hexagonal mesoporous silica strands	Separation of silver nanoparticles
65	F127	1 : 0.02 : 32 : 0.3 : 11	18 h; 60 °C	RT (4 mL dropped) (5 min drying)	Nanotubes	Gas permeation experiments
66	CTAB P123 Brij 98	1 : 0.2 : 17 : 3 1 : 0.01 : 17 : 3 1 : 0.1 : 17 : 3	—	<0.04 MPa	Hexagonal mesocylinder structures	Separation of high concentration macromolecules *e.g.* insulin, α-amylase, β-lactoglobulin, and myosin
67	F108	1 : 0.007 : 17 : 3	—	<0.04 MPa	3D mesocage structures	Separation of cytochrome c (CytC), myoglobin (Mb) and haemoglobin (Hb)
Dip-coating & magnetic field induction						
68	P123	1 : 0.01 : 9 : 3	3 h; RT	2 h; RT; 30 T	2D hexagonally ordered mesochannels, circularly packed around the alumina channel	/
Vapour-deposition hydrolysis						
27	CTAB	— : 0.008 : 0.05 : 0.008 : 1	—	3 h; 100 °C	Parallel alignment of mesostructure, changes to tilted alignment when alkyl chain of surfactant length is decreased	/
69	CTAB P123 F127	1 : 3 : 0 : 0.7 : 0 1 : 0.2 : 0 : 0.7 : 0 1 : 0.07 : 0 : 0.7 : 0	—	(1 mL) RT; 2 h; 100 °C	CTAB → circular hexagonal phase P123 → reversed circular hexagonal phase F127 → body centered cubic phase	
Electrodeposition & dip-coating						
70	P123	1 : 0.16 : 379 : 8 : 10	1 h; 60 °C; 2 h	3–18 h; 0.3, 2.3, 5 V	Increased electric field → nanotubules to more completely filled nanorod structures Deposition time > 7 h → preferential axial alignment of pores, nanorods uniformly filled	/
71	CTAB	1 : 0.3 : 0.03 : 0.001 : 6	2.5 h; RT	RT	Nanorods of mesoporous structure with pore size distribution of 2.0–3.8 nm	/

[a] — = information not provided; / = no application; * = THT-based sol; RT = room temperature.

Alternative methods that have also been employed in the fabrication of MS–AAM include electrodeposition and vapour-deposition. The electrodeposition of mesoporous silica fibres using AAM as a hard template was reported by Hill's and Ren's groups.[70,71] Silica sol was deposited within AAM channels mounted on electrodes connected to a DC power supply, followed by hydrolysis in air. The applied electric field was found to strongly affect the structure and orientation of the nanorods within the AAM channels, with ordered pores oriented axially, apparent when a bias of 5 V was applied over 7 h. With the vapour-phase synthesis (VPS) approach, infiltration of a surfactant solution into the AAM pores was carried out first. Then, the AAM was placed in a sealed container where vaporized silica molecules diffuse into the self-assembled surfactant structure. In a first report by Jang's group,[27] the surfactant solution was introduced into the AAM pores by immersion, leading to the formation of an undesirable mesoporous silica layer on the external alumina membrane surface. In a more recent report, Guo *et al.*[72] infiltrated the surfactant solution into the AAM channels under a reduced pressure to avoid the residual layer on the AAM external surface. Then, the AAM was treated by VPS to produce a silica–AAM composite. The results showed that ordered mesostructures are formed at higher concentration ratios of surfactant to acid solution. For CTAB-templated samples, a columnar hexagonal phase was observed, as expected, but the circular hexagonal phase was also demonstrated for a sample with surfactant to acid solution mass ratio of 0.24. This differs from previous reports where only the columnar hexagonal phase was seen. The pore diameter of the mesoporous silica formed was determined to be *ca.* 2.7 nm. The F127-templated samples formed cubic ordered mesoporous structures with large cage-like pores of *ca.* 12 nm in diameter, at 100 °C and irrespective of the concentration ratio. The P123-templated samples produced a combination of inverse columnar hexagonal and tubular thick lamellar structures of *ca.* 8 nm in diameter. At low concentration, disordered lamellar mesostructures were seen. Keeping the concentration of surfactant fixed at 30%, tubular lamellar structures were obtained at 60 °C, inverse hexagonal circular structures (incomplete and less ordered) at 80 °C, and closely packed silica nanoparticles within a silica nanotube at 120 °C. Most interestingly, for the samples with ordered mesostructures, excellent filling of mesoporous silica within the AAM pores was reported with no slits or gaps between the AAM pore walls and silica. The higher surfactant concentration and higher temperature (100 °C, which is higher than the temperature used in the EISA method), was said to account for the increased filling.

The majority of the reported investigations in Table 1 removed the alumina matrix after synthesis of the mesoporous silica fibres, by dissolving it in an acidic solution, to obtain the residual silica nanomaterial. Only a few investigators, including Yamaguchi *et al.* and El-Safty *et al.*, have applied the MS–AAM composite membrane itself. Shi *et al.*[40] immobilized lysine onto the MS–AAM composite membrane and used it as an affinity membrane to adsorb bilirubin from a bilirubin–phosphate solution and bilirubin–albumin solution. The composite membrane has also been used as a template to fabricate nanorods of other materials,[1,51] for drug adsorption and release experiments,[49] and as a filter for the separation of macromolecules.[63,64,66]

In summary, there is now an extensive literature on the synthesis, characterization and morphology of silica mesostructures. However, the formation of a robust hybrid composite mesoporous silica–anodic alumina membrane (MS–AAM) to carry out selective separations is still a challenge. Despite many investigations on MS–AAM, very few sought to form a membrane. For this purpose, it is critical to synthesize a crack-free nanoporous membrane in which the channels of the macroporous support (AAM) are tightly filled with nanoporous material (MS). In the remainder of this paper, we discuss the challenges associated with the preparation of such a membrane, comparing and extending several of the reported synthesis methods.

2. Experimental

2.1. Materials

Tetraethyl orthosilicate (TEOS, reagent grade 98%), hydrochloric acid (HCl, ACS reagent 37 wt%), ethanol (EtOH, anhydrous ≥99.5 wt%), and Pluronic P-123 (EO_{20}–PO_{70}–EO_{20}; EO = ethylene oxide, PO = propylene oxide), were obtained from Sigma. All chemicals were used as-received without any further purification. Anodic alumina membranes (AAM, Whatman) with a 25 mm diameter, an average channel diameter of 200 nm and a thickness of approximately 60 μm, were used as purchased. Some membranes were modified using an oxygen plasma.

2.2. Synthesis of mesostructured silica within AAM channels

To synthesize mesostructured silica within the channels of AAM, a silica precursor sol solution is introduced into the AAM pores *via* a number of different routes, with the formation mechanism shown in Fig. 1.

Aspiration. The precursor sol was prepared based on the work of Yamaguchi and co-workers.[59] First, 1.0 g of P123 was dissolved in a mixture of 15 g of EtOH, 0.1 g of concentrated HCl solution (12 M) and 2.0 g of H_2O. This mixture was stirred for 1 h under reflux. Then, 2.13 g of TEOS was added dropwise to the mixture, and stirring was continued at 60 °C for 7–16 h. In some cases, 0.42 g of sodium chloride (NaCl) salt was added (Fig. 2).

The AAM was set in a membrane filtration apparatus and 4–10 mL of the precursor solution was dropped onto the alumina membrane. Penetration of the silica sol was achieved by means of vacuum at a pressure ≤ 20 kPa. The membrane was dried under aspiration for 5 min at room temperature and calcined at 500 °C for 5 h to remove the surfactant template.

Sol–gel (rotary). This method followed the work of Yao and co-workers.[35] 10.4 g of TEOS, 25 g of EtOH, 1 g of HCl (1 M) and 5 g of P123 were mixed together and stirred at 37 °C for 10 min until a clear solution was formed. The alumina membrane was immersed in the as-prepared sol and a rotary evaporator in vacuum condition evaporated all of the volatile solvent at 40 °C for 25 min. Some samples were aged in the remaining sol at 60

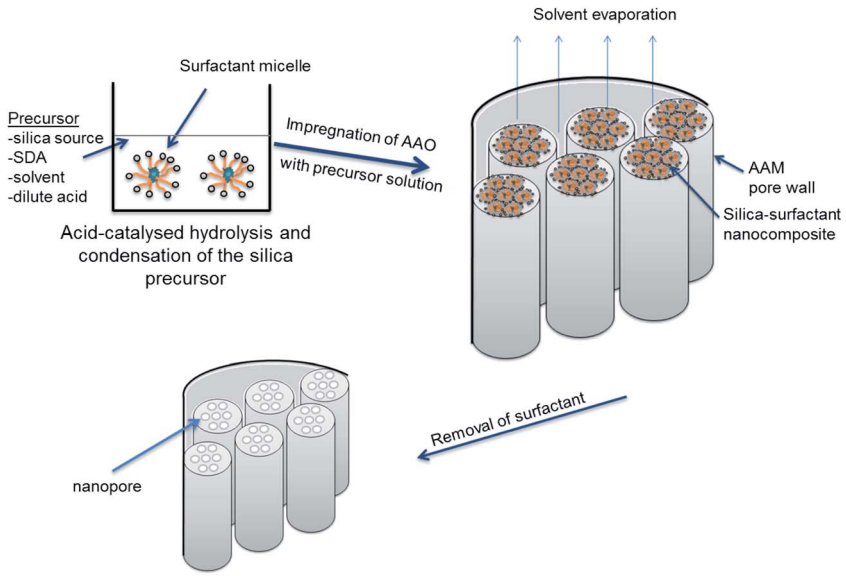

Fig. 1 Formation mechanism of hybrid silica–alumina composite membrane.

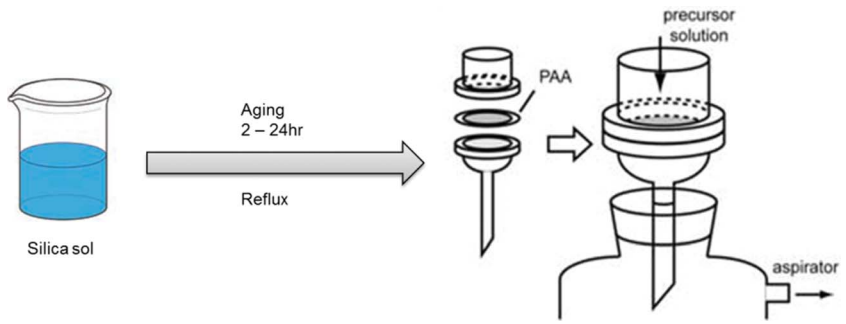

Fig. 2 Schematic illustration of aspiration procedure (adapted from ref. 59).

°C for 12 h, while other ones were aged outside of the sol at 60 °C for 12 h. The surfactant template was removed by treating at high temperature (540 °C) for 6 h or by carrying out ethanol extraction at 70 °C for 6 h.

Sol–gel (multi-stage). The precursor solution was prepared based on the procedure of Zhao and co-workers.[4] 1 g of P123 was dissolved in a mixture of 5 g of EtOH and 0.2 g of HCl (1 M). After forming a clear solution, 2.08 g of TEOS was added and stirred for 10 min. The composite membrane was fabricated according to the literature,[33] with some modifications. The alumina membrane was immersed in the silica sol for 10 min. Excess sol was wiped off. An evaporation-driven gelation period was carried out for 3 h at room temperature. The as-synthesized membrane was calcined at 500 °C for 4 h. The membrane was recycled through the process up to four times. Subsequent calcinations were carried out at 400 °C for 4 h, with the membrane held between two porous plates (Fig. 3).

Sol–gel (dip-coating). To prepare the precursor solution, a silica solution and surfactant solution were made separately. First, 2.08 g of TEOS was mixed with 3 g of HCl (0.2 M), 1.8 g of deionized H_2O and 5 mL EtOH, for 1 h at 60 °C. For the preparation of the surfactant solution, 0.75 g of P123 was mixed with 15 mL of EtOH and stirred at room temperature until clear. Both solutions were mixed together and stirred further at room temperature for 2, 4 and 6 h. Whatman Anodisc 25 membrane was dipped into each precursor sol by attaching the membrane to a clamp and withdrawing vertically from the sol reservoir. The speed of withdrawal was set at 0.2 mm s^{-1}. To remove the surfactant, the membrane was calcined at 500 °C for 4 h.

2.3. Materials characterization

Field emission scanning electron microscopic (FESEM) images were obtained with a Zeiss SUPRA 55 microscope. The membrane samples were coated with a thin platinum layer and fixed on the FESEM stage using carbon tapes. Small angle X-ray scattering patterns were obtained using a Bruker Nanostar. The composite membranes were ground into a fine powder. Nitrogen adsorption–desorption measurements were carried out at 77 K with an Autosorb iQ pore size analyser (Quantachrome Instruments, Florida, USA). Samples were ground into a fine powder and placed inside a 6 mm tube. The specific surface

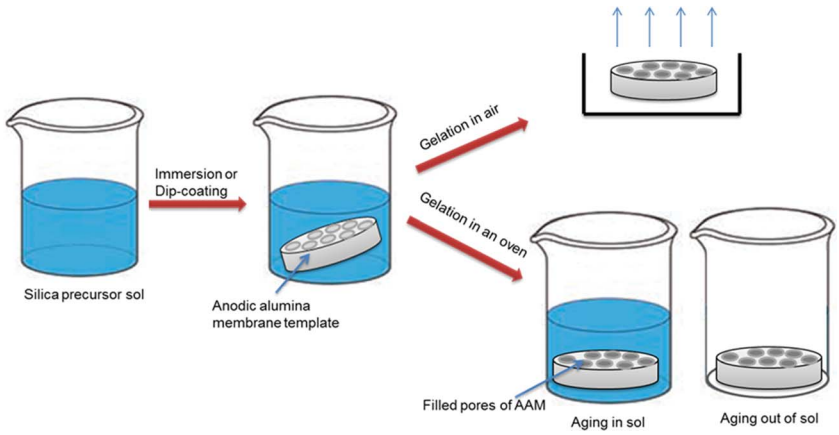

Fig. 3 Schematic illustration of sol–gel procedure (adapted from ref. 15).

area and the pore size distribution were calculated according to the Brunauer–Emmett–Teller (BET) and Barrett–Joyner–Halenda (BJH) model, respectively, using the adsorption branch of the isotherm. The surface areas quoted below are in m^2 per gram of AAM, *i.e.*, they include the anodic alumina.

3. Results and discussion

The fabrication of silica mesostructures within the channels of AAM from ethanol-based precursor solutions was carried out *via* the four described routes. The results from these studies draw attention to key challenges encountered in the formation of silica–AAM composites.

3.1. Partial filling of AAM channels

SEM images were taken to obtain information about the mesoporous silica rods within the AAM channels. Partial filling, where some but not all of the alumina channels contain mesoporous silica, was repeatedly observed. Fig. 4 shows typical FESEM images of a silica–AAM composite prepared by the sol–gel method. A majority of the alumina pores seen in Fig. 4a are empty with a few possibly containing silica, indicated by the lighter dense grey colour seen inside the pores. Fig. 4b shows alumina pores in the centre that appear to contain silica, but a good portion of the alumina matrix is not filled with silica material.

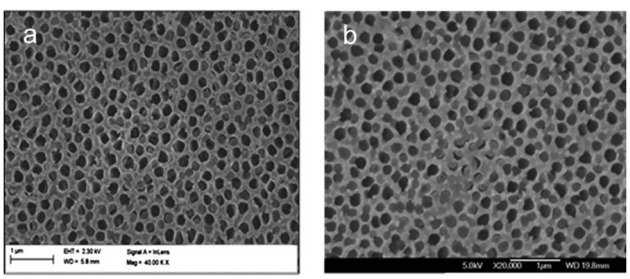

Fig. 4 FESEM images of silica–AAM composites formed by the sol–gel method with rotary evaporation.

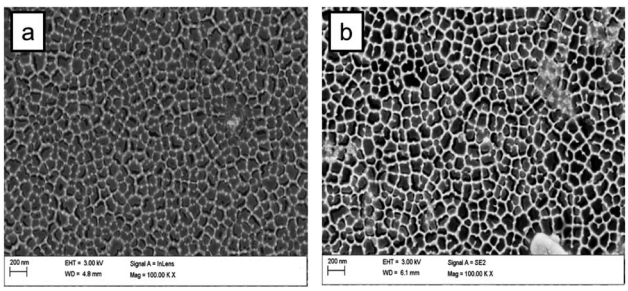

Fig. 5 FESEM images of silica–AAM composites formed by aspiration at (a) 20 kPa and (b) 30 kPa.

Encouraging results were obtained with the aspiration method. The vacuum pressure was varied to determine its effect on pore filling. Fig. 5a shows almost complete filling when aspiration was carried out at 20 kPa. By comparison, a higher vacuum pressure leaves more alumina pores empty, as seen in Fig. 5b. A potential risk with this method is that a high aspiration rate could suck the solution quickly through the alumina membrane pores leaving insufficient time for nucleation and growth.

Partial filling is a problem that greatly affects the quality and effectiveness of the composite membrane. If some of the channels of the AAM remain even partially open, leaving gaps wider than the silica mesopores, undesired components in solution can easily be transported across the membrane. The observed poor filling is confirmed by TEM and SEM images shown in many of the aforementioned articles. For example, Platschek *et al.*[44] reported that 30% of the AAM pores were empty after infiltration of silica precursor solution and calcination, and, in another study, it was determined that only ~20% of the alumina channels were filled with silica structures.[52] El-Safty *et al.*[62,63,66] fabricated hybrid membranes with air-tight silica nanotubes, with large domain sizes of a uniform, ordered structure. However, the TEM images still showed several AAM pores that appeared empty. Even though some studies reported that the AAM pores were completely filled, the results were only based on the synthesized mesostructured

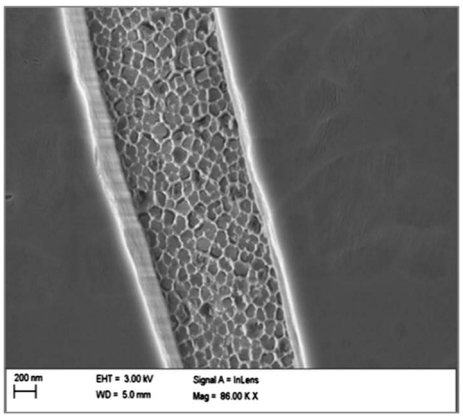

Fig. 6 FESEM image of a silica–AAM composite formed by a three-times repeated multi-stage sol–gel method.

silica arrays obtained after the complete dissolution of the alumina matrix. Moreover, reports that proposed solutions to the partial filling problem did not show any transport data to support their claim. Therefore, complete filling is hard to ascertain.

3.2. Overgrowth of silica on the external AAM Surface

We also note that procedures using the sol–gel method often result in the formation of a silica layer on the external surface of the alumina membrane. A possible cause is that, during immersion, a gel phase is grown on both sides of the AAM, which results in an overlayer. In Fig. 6, a top view of a composite membrane formed by the multistage process is shown. A silica overlayer is seen with a narrow strip between the layers, showing, what appear to be, filled alumina pores. Formation of a silica overlayer is also observed when dip-coating is used as the method of fabrication. A thin film of silica is deposited on top of the membrane surface. Formation of this silica layer on the external alumina membrane surface blocks the alumina pores, interfering with the use of the membrane for transport-based separation processes.

Several attempts were made to remove the silica top layer, including etching with hydrofluoric (HF) acid, immersing in potassium hydroxide (KOH) and lightly scratching away the top

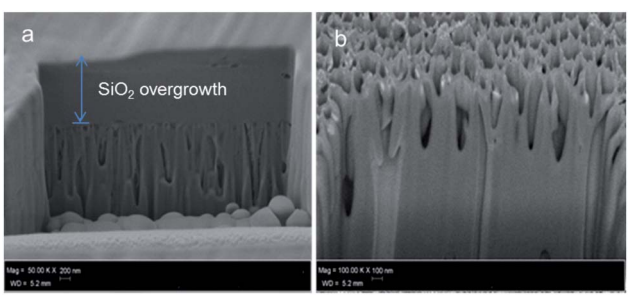

Fig. 7 Cross-sectional FESEM images of a silica–AAM composite membrane synthesized by (a) four-times repeated (multistage) sol–gel method; (b) aspiration.

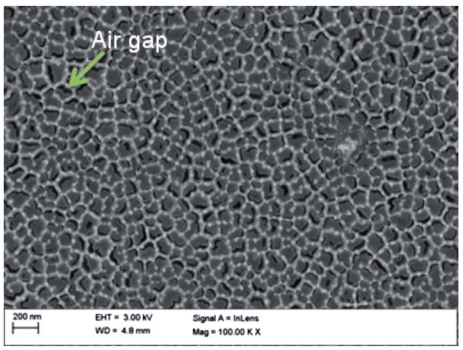

Fig. 8 FESEM image of silica–AAM synthesized by aspiration, showing silica shrinkage after calcination.

alumina surface with a razor blade under an optical microscope. These methods are destructive and invasive. HF or any other solution will etch away the top but may also enter the alumina channels and alter the silica material inside the channels of the AAM. Scraping the membrane, even lightly, breaks and damages its structure. Either of these scenarios decreases the performance of the membrane. To the best of our knowledge, successful attempts have not yet been demonstrated.

The aspiration method, proposed by Yamaguchi *et al.*[55,59] counters the overgrowth problem. Yamaguchi *et al.* hypothesized that, since the silica precursor solution is introduced into the columnar alumina channels by pressure, this leaves little or no formation of mesoporous silica on the external alumina membrane surface. This is the preferred state for applications in mass-transport driven separation systems. The multistage sol–gel method, which should deposit more silica within the AAM channels and, thereby, improve the pore filling unfortunately also tends to increase the silica overgrowth, as seen in Fig. 7a. The height of the silica overgrowth layer is roughly indicative of the number of immersion times. In contrast, the composite membrane shown in Fig. 7b shows no silica layer on the external membrane surface.

3.3. Removal of surfactant

Calcination and solvent extraction are two methods commonly used for surfactant removal. Removal of the surfactant template by calcination causes the silica material to contract and shrink away from the alumina channel walls. This creates gaps between the mesoporous silica rods or nanotubes and the inner surface of the AAM pore channels (Fig. 8). These gaps negatively affect the selective transport of molecules through the hybrid composite membrane.

Removal of the surfactant template by solvent extraction may preserve the structural integrity of the silica material within the alumina channels. With this method, the air gaps that usually form during calcination are avoided. However, special care is required for this process, when using Whatman membranes, such as ensuring that, after the procedure, the filtration side of the membrane surface is retrieved and the membrane is still intact for subsequent use. El-Safty's group[61,66,73] created strong

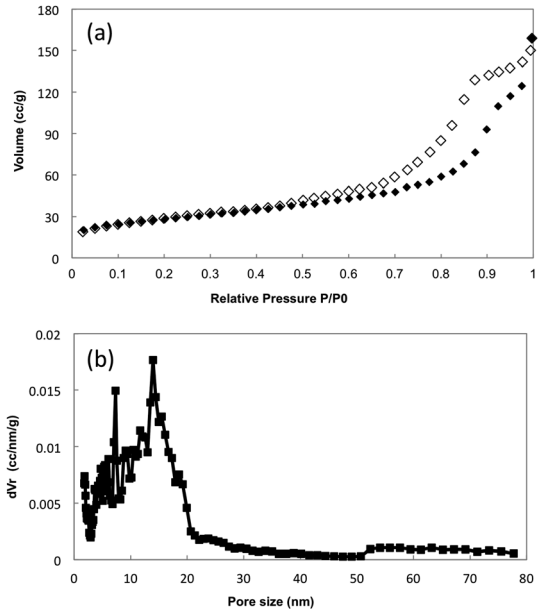

Fig. 9 (a) Nitrogen adsorption (solid symbols) and desorption (open symbols) isotherms; (b) pore size distribution of a silica–AAM composite formed by a three-times (multistage) sol–gel method.

interactions between the silica–surfactant composites and the AAM channel walls by attaching TMAC linkers to the alumina wall. They proposed that the TMAC–AAM walls facilitated the formation of rigid silica nanotubes. In another step in their fabrication procedure, trimethylsilane (TMS) was grafted onto the formed silica nanotubes to prevent shrinkage during the calcination step and also to preserve the silica inner pore structure during separation assays under pressure.

3.4. Reproducibility of experimental results

The results are very sensitive to the synthesis conditions applied during the different fabrication methods. Slight changes in the silica-to-surfactant composition ratio, the humidity, the vacuum pressure or the temperature during the aging step lead to very big (and negative) changes in the filling of the alumina channels and the structure and order of the silica nanochannels. Obtaining ordered silica arrays has also been difficult, even when following well-documented procedures.

Nitrogen adsorption and desorption measurement results, shown in Fig. 9, display a type IV behaviour typical of mesoporous materials. The pore size distribution is much broader than expected, but centered around 14 nm. Subsequent SAXS measurement of samples prepared by the same procedure showed no characteristic peaks that would be indicative of long-range order. It is interesting to note that SAXS measurements performed on the same precursor solution cast on a thin quartz slide yielded patterns indicative of an ordered structure. The same was seen for the aspiration-formed composite membrane samples. This suggests that either the silica pores are not ordered inside the AAM channels, a larger quantity of sample is needed, or the order is too short-ranged to be revealed by SAXS.

3.5. Hard template

Alumina channels are a good choice for the hard template because they have vertical channels that will lead to the formation of vertically aligned silica nanochannels. However, Whatman Anodisc membranes are very fragile and brittle, hence they are difficult to handle. After calcination, the polypropylene ring bonded to the membrane for ease of handling is burned off, adding to the difficulties of using these materials for separation experiments. Other alumina membranes were used, which are the Synkera anodic alumina membranes and alumina membranes provided by the group of Dr. J. Lutkenhaus, Texas A&M, USA. These membranes have monodispersed pores with a diameter of 150 nm and 40 nm, respectively. Although more mechanically robust, the same challenges outlined above were observed with these membranes. This suggests that the common factor in all these membranes is the surface chemistry of the alumina membranes, which is likely to be the problem.

Modifying the alumina membrane surface so that it bonds more easily to silica will lead to stronger attachment between the silica arrays and the alumina channel walls. This will also improve the filling degree and possibly solve the air gap issue. Keller *et al.*[54] recently investigated the influence of wall chemistry on the silica orientation. As stated in their report, increasing the negative charge on the alumina channel surface delays the silica condensation and leads to an abundance of the vertically aligned phase. Their TEM images show almost complete filling of the entire alumina channels. The best results could likely be obtained by combining modification of the alumina wall chemistry with the right fabrication method.

4. Conclusion

Fabricating a mesoporous silica–anodic alumina composite membrane is not a trivial endeavour, and more challenging than electron microscopy images on small areas suggest. It requires attention to every synthesis parameter to ensure that the AAM channels are filled tightly with silica throughout the membrane, over macroscopic distances. For these same reasons, reproducing the synthesis of a composite membrane consisting of mesoporous silica and anodic alumina remains difficult. It is clear that, for most experimental reports in the literature, the authors had different objectives, such as the study of different silica mesophases, or the release of adsorbed molecules. In these applications, the anodic alumina was only vital to the formation of the silica material and not for its final use as a membrane. In addition, the majority of these studies used commercially available Whatman anodic alumina membranes that are very brittle and fragile in nature. Extreme care is required to ensure successful experimental procedures. It is also necessary to alter the surface chemistry of the alumina membrane to successfully grow dense and rigid silica nanochannels.

The aspiration technique appears to be the most effective method for preparing a mesostructured silica–AAM composite membrane that can be used as a nano-filter. Although several

others have successfully synthesized ordered mesoporous silica inside AAM channels, there remains insufficient published evidence on the use of such a material as a membrane, as well as a limited understanding on the time scales of the growth of the silica–surfactant structures within the alumina channels. Among the published evidence, El-Safty *et al.* and Yamaguchi *et al.* have demonstrated interesting preliminary results that provide information regarding the potential use of this composite membrane for separation applications. However, these are only the first steps toward the creation of membranes that have the required mechanical and transport characteristics for long-term permeation in practical applications.

Acknowledgements

The authors acknowledge and are grateful for funding provided by the United States National Science Foundation *via* the NSF EAGER Program of the CBET Chemical & Biological Separations Division, CBET-104920 as well as CBET-0967937. Part of this work was carried out at the Department of Chemical & Biological Engineering, Rensselaer Polytechnic Institute, USA. The authors also gratefully acknowledge the EPSRC of the UK for continued funding *via* a "Frontier Engineering" Award, EP/K038656/1, to the Centre for Nature Inspired Engineering at UCL. Underlying research data can be accessed *via* the authors.

References

1 G. Ji, Z. Gong, Y. Liu, X. Chang, Y. Du and M. Qamar, Fabrication and Magnetic Properties of Cobalt Nanorod Arrays Containing a Number of Ultrafine Nanowires Electrodeposited Within an AAO/SBA-15 Template, *Solid State Commun.*, 2011, **151**, 1151–1155.

2 J. Li, Y. Zhang, Y. Hao, J. Zhao, X. Sun and L. Wang, Synthesis of Ordered Mesoporous Silica Membrane on Inorganic Hollow Fiber, *J. Colloid Interface Sci.*, 2008, **326**, 439–444.

3 A. Vinu, T. Mori and K. Ariga, New Families of Mesoporous Materials, *Sci. Technol. Adv. Mater.*, 2006, **7**, 753–771.

4 H. Yang, Q. Shi, B. Tian, S. Xie, F. Zhang, Y. Yan, B. Tu and D. Zhao, A Fast Way for Preparing Crack-Free Mesostructured Silica Monolith, *Chem. Mater.*, 2003, **15**, 536–541.

5 D. Zhao, Q. Huo, J. Feng, B. F. Chmelka and G. D. Stucky, Nonionic Triblock and Star Diblock Copolymer and Oligomeric Surfactant Syntheses of Highly Ordered, Hydrothermally Stable, Mesoporous Silica Structures, *J. Am. Chem. Soc.*, 1998, **120**, 6024–6036.

6 T. Yamada, H. Zhou, K. Asai and I. Honma, Pore Size Controlled Mesoporous Silicate Powder Prepared by Triblock Copolymer Templates, *Mater. Lett.*, 2002, **56**, 93–96.

7 J. S. Beck, J. C. Vartuli, W. J. Roth, M. E. Leonowicz, C. T. Kresge, K. D. Schmitt, C. T.-W. Chu, D. H. Olson, E. W. Sheppard, S. B. McCullen, J. B. Higgins and J. L. Schlenker, A New Family of Mesoporous Molecular Sieves Prepared with Liquid Crystal Templates, *J. Am. Chem. Soc.*, 1992, **114**, 10834–10843.

8 C. T. Kresge, M. E. Leonowicz, W. J. Roth, J. C. Vartuli and J. S. Beck, Ordered Mesoporous Molecular Sieves Synthesized by a Liquid-crystal Template Mechanism, *Nature*, 1992, **359**, 710–712.

9 P. Innocenzi, L. Malfatti, T. Kidchob and P. Falcaro, Order–Disorder in Self-Assembled Mesostructured Silica Films: A Concepts Review, *Chem. Mater.*, 2009, **21**, 2555–2564.

10 J. E. Martin, M. T. Anderson, J. Odinek and P. Newcomer, Synthesis of Periodic Mesoporous Silica Thin Films, *Langmuir*, 1997, **7463**, 4133–4141.

11 W. Zhu, Y. Han and L. An, Synthesis of Ordered Mesostructured Silica Nanotubal Arrays, *Microporous Mesoporous Mater.*, 2005, **84**, 69–74.

12 P. Kohli and C. R. Martin, Smart Nanotubes for Biotechnology, *Curr. Pharm. Biotechnol.*, 2005, **6**, 35–47.

13 M. Zhang, Y. Bando, K. Wada and K. Kurashima, Synthesis of Nanotubes and Nanowires of Silicon Oxide, *J. Mater. Sci. Lett.*, 1999, **18**, 1911–1913.

14 C. J. Brinker, Y. Lu, A. Sellinger and H. Fan, Evaporation-Induced Self-Assembly: Nanostructures Made Easy, *Adv. Mater.*, 1999, **11**, 579–585.

15 B. Platschek, A. Keilbach and T. Bein, Mesoporous Structures Confined in Anodic Alumina Membranes, *Adv. Mater.*, 2011, **23**, 2395–2412.

16 M. Mesa, L. Sierra and J.-L. Guth, Contribution to the Study of the Formation Mechanism of Mesoporous SBA-15 and SBA-16 Type Silica Particles in Aqueous Acid Solutions, *Microporous Mesoporous Mater.*, 2008, **112**, 338–350.

17 L. G. A. van de Water and T. Maschmeyer, Mesoporous Membranes—A Brief Overview of Recent Developments, *Top. Catal.*, 2004, **29**, 67–77.

18 R. K. Iler, *The Chemistry of Silica: Solubility, Polymerization, Colloid and Surface Properties, and Biochemistry*, John Wiley & Sons, New York, 1979.

19 C. J. Brinker, Hydrolysis and Condensation of Silicates: Effects on Structure, *J. Non-Cryst. Solids*, 1988, **100**, 31–50.

20 D. Zhao, P. Yang, N. Melosh, J. Feng, B. F. Chmelka and G. D. Stucky, Continuous Mesoporous Silica Films with Highly Ordered Large Pore Structures, *Adv. Mater.*, 1998, **10**, 1380–1385.

21 M. Klotz, P.-A. Albouy, A. Ayral, C. Ménager, D. Grosso, A. Van der Lee, V. Cabuil, F. Babonneau and C. Guizard, The True Structure of Hexagonal Mesophase-Templated Silica Films As Revealed by X-ray Scattering: Effects of Thermal Treatments and of Nanoparticle Seeding, *Chem. Mater.*, 2000, **12**, 1721–1728.

22 C. R. Martin, Membrane-Based Synthesis of Nanomaterials, *Chem. Mater.*, 1996, **8**, 1739–1746.

23 J. C. Hulteen and C. R. Martin, A General Template-based Method for the Preparation of Nanomaterials, *J. Mater. Chem.*, 1997, **7**, 1075–1087.

24 G. Kickelbick, Formation of Hexagonal Mesoporous Silica in Submicrometer Channels, *Small*, 2005, **1**, 168–170.

25 Y. Wu, T. Livneh, Y. X. Zhang, G. Cheng, J. Wang, J. Tang, M. Moskovits and G. D. Stucky, Templated Synthesis of Highly Ordered Mesostructured Nanowires and Nanowire Arrays, *Nano Lett.*, 2004, **4**, 2337–2342.

26 K. Jin, B. Yao and N. Wang, Structural Characterization of Mesoporous Silica Nanowire Arrays Grown in Porous Alumina Templates, *Chem. Phys. Lett.*, 2005, **409**, 172–176.

27 K. J. Lee, S. H. Min and J. Jang, Vapor-phase Synthesis of Mesostructured Silica Nanofibers Inside Porous Alumina Membranes, *Small*, 2008, **4**, 1945–1949.

28 Z. Gong, G. Ji, M. Zheng, X. Chang, W. Dai, L. Pan, Y. Shi and Y. Zheng, Structural Characterization of Mesoporous Silica Nanofibers Synthesized Within Porous Alumina Membranes, *Nanoscale Res. Lett.*, 2009, **4**, 1257–1262.

29 Z. Yang, Z. Niu, X. Cao, Z. Yang, Y. Lu, Z. Hu and C. C. Han, Template Synthesis of Uniform 1D Mesostructured Silica Materials and Their Arrays in Anodic Alumina Membranes, *Angew. Chem., Int. Ed.*, 2003, **42**, 4201–4203.

30 C. R. Martin and Z. Siwy, Molecular Filters – Pores Within Pores, *Nat. Mater.*, 2004, **3**, 284–285.

31 D. T. Mitchell, S. B. Lee, L. Trofin, N. Li, T. K. Nevanen, H. Söderlund and C. R. Martin, Smart Nanotubes for Bioseparations and Biocatalysis, *J. Am. Chem. Soc.*, 2002, **124**, 11864–11865.

32 Q. Lu, F. Gao, S. Komarneni and T. E. Mallouk, Ordered SBA-15 Nanorod Arrays Inside a Porous Alumina Membrane, *J. Am. Chem. Soc.*, 2004, **126**, 8650–8651.

33 A. Y. Ku, S. T. Taylor and S. M. Loureiro, Mesoporous Silica Composites Containing Multiple Regions with Distinct Pore Size and Complex Pore Organization, *J. Am. Chem. Soc.*, 2005, **127**, 6934–6935.

34 M. Zhang, Y. Bando and K. Wada, Silicon Dioxide Nanotubes Prepared by Anodic Alumina as Templates, *J. Mater. Res.*, 2000, **15**, 387–392.

35 B. Yao, D. Fleming, M. A. Morris and S. E. Lawrence, Structural Control of Mesoporous Silica Nanowire Arrays in Porous Alumina Membranes, *Chem. Mater.*, 2004, **16**, 4851–4855.

36 Y. Wu, G. Cheng, K. Katsov, S. W. Sides, J. Wang, J. Tang, G. H. Fredrickson, M. Moskovits and G. D. Stucky, Composite Mesostructures by Nano-confinement, *Nat. Mater.*, 2004, **3**, 816–822.

37 S. Yoo, D. M. Ford and D. F. Shantz, Synthesis and Characterization of Uniform Alumina–Mesoporous Silica Hybrid Membranes, *Langmuir*, 2006, **22**, 1839–1845.

38 A. Y. Ku, S. T. Taylor, W. J. Heward, L. Denault and S. M. Loureiro, Heterogeneous Mesoporous Oxides Grown in Porous Anodic Alumina, *Microporous Mesoporous Mater.*, 2006, **88**, 214–219.

39 Y. Yamauchi, T. Nagaura and S. Inoue, Oriented Growth of Small Mesochannels Utilizing a Porous Anodic Alumina Substrate: Preparation of Continuous Film with Standing Mesochannels, *Chem.–Asian J.*, 2009, **4**, 1059–1063.

40 W. Shi, Y. Shen, H. Jiang, C. Song, Y. Ma, J. Mu, B. Yang and D. Ge, Lysine-attached Anodic Aluminum Oxide (AAO)–silica Affinity Membrane for Bilirubin Removal, *J. Membr. Sci.*, 2010, **349**, 333–340.

41 E.-M. Kim, J.-S. Jung and W.-S. Chae, Interfacial Interaction Induced Mesostructural Changes in Nanocylinders, *Chem. Commun.*, 2010, **46**, 1760–1762.

42 M. N. Jalil, H. M. Zaki, R. A. W. Dryfe and M. W. Anderson, Porosity Study of Hybrid Silica Mesostructure in Aluminium Oxide Membrane Columnar by Cyclic Voltammetry Method, *Journal of Science and Technology*, 2011, **3**, 43–50.

43 A. Zhang, K. Hou, L. Gu, C. Dai, M. Liu, C. Song and X. Guo, Synthesis of Silica Nanotubes with Orientation Controlled Mesopores in Porous Membranes *via* Interfacial Growth, *Chem. Mater.*, 2012, **24**, 1005–1010.

44 B. Platschek, N. Petkov and T. Bein, Tuning the Structure and Orientation of Hexagonally Ordered Mesoporous Channels in Anodic Alumina Membrane Hosts: a 2D Small-angle X-ray Scattering Study, *Angew. Chem., Int. Ed.*, 2006, **45**, 1134–1138.

45 N. Petkov, B. Platschek, M. A. Morris, J. D. Holmes and T. Bein, Oriented Growth of Metal and Semiconductor Nanostructures Within Aligned Mesoporous Channels, *Chem. Mater.*, 2007, **19**, 1376–1381.

46 B. Platschek, R. Köhn, M. Döblinger and T. Bein, Formation Mechanism of Mesostructured Silica in Confined Space: An In Situ GISAXS Study, *ChemPhysChem*, 2008, **9**, 2059–2067.

47 B. Platschek, N. Petkov, D. Himsl, S. Zimdars, Z. Li, R. Köhn and T. Bein, Vertical Columnar Block-copolymer-templated Mesoporous Silica *via* Confined Phase Transformation, *J. Am. Chem. Soc.*, 2008, **130**, 17362–17371.

48 B. Platschek, R. Köhn, M. Döblinger and T. Bein, In Situ GISAXS Study of the Formation of Mesostructured Phases Within the Pores of Anodic Alumina Membranes, *Langmuir*, 2008, **24**, 5018–5023.

49 V. Cauda, L. Mühlstein, B. Onida and T. Bein, Tuning Drug Uptake and Release Rates through Different Morphologies and Pore Diameters of Confined Mesoporous Silica, *Microporous Mesoporous Mater.*, 2009, **118**, 435–442.

50 A. Keilbach, M. Döblinger, R. Köhn, H. Amenitsch and T. Bein, Periodic Mesoporous Organosilica in Confined Environments, *Chem.–Eur. J.*, 2009, **15**, 6645–6650.

51 A. Keilbach, J. Moses, R. Köhn, M. Döblinger and T. Bein, Electrodeposition of Copper and Silver Nanowires in Hierarchical Mesoporous Silica/Anodic Alumina Nanostructures, *Chem. Mater.*, 2010, **22**, 5430–5436.

52 A. Keller, S. Kirmayer, T. Segal-Peretz and G. L. Frey, Mesostructured Silica Containing Conjugated Polymers Formed Within the Channels of Anodic Alumina Membranes from Tetrahydrofuran-based Solution, *Langmuir*, 2012, **28**, 1506–1514.

53 N. Gargiulo, I. De Santo, F. Causa, D. Caputo and P. A. Netti, Confined Mesoporous Silica Membranes for Albumin Zero-order Release, *Microporous Mesoporous Mater.*, 2013, **167**, 71–75.

54 A. Keller, T. Segal-Peretz, Y. Kauffmann and G. L. Frey, Control over In-channel Mesostructure Orientation through AAM Surface Modification, *Phys. Chem. Chem. Phys.*, 2013, **15**, 13637–13645.

55 A. Yamaguchi, F. Uejo, T. Yoda, T. Uchida, Y. Tanamura, T. Yamashita and N. Teramae, Self-assembly of a Silica–Surfactant Nanocomposite in a Porous Alumina Membrane, *Nat. Mater.*, 2004, **3**, 337–341.

56 T. Yamashita, S. Kodama, M. Ohto, E. Nakayama, S. Hasegawa, N. Takayanagi, T. Kemmei, A. Yamaguchi, N. Teramae and Y. Saito, Permeation Flux of Organic Molecules through Silica–Surfactant Nanochannels in a Porous Alumina Membrane, *Anal. Sci.*, 2006, **22**, 1495–1500.
57 A. Yamaguchi, J. Watanabe, M. M. Mahmoud, R. Fujiwara, K. Morita, T. Yamashita, Y. Amino, Y. Chen, L. Radhakrishnan and N. Teramae, Extraction Mechanisms of Charged Organic Dye Molecules into Silica–Surfactant Nanochannels in a Porous Alumina Membrane, *Anal. Chim. Acta*, 2006, **556**, 157–163.
58 A. Yamaguchi, T. Yoda, S. Suzuki, K. Morita and N. Teramae, Diffusivities of Tris(2,2′-bipyridyl)ruthenium Inside Silica-nanochannels Modified with Alkylsilanes, *Anal. Sci.*, 2006, **22**, 1501–1507.
59 A. Yamaguchi, H. Kaneda, W. Fu and N. Teramae, Structural Control of Surfactant-Templated Mesoporous Silica Formed Inside Columnar Alumina Pores, *Adv. Mater.*, 2008, **20**, 1034–1037.
60 L. Radhakrishnan, A. Yamaguchi, W. Fu, H. Kaneda and N. Teramae, Integration of Mesostructured Silica with Bathophenanthroline into a Porous Alumina Membrane by One-pot Synthesis Method, *Microporous Mesoporous Mater.*, 2008, **113**, 139–145.
61 S. A. El-Safty, A. Shahat, M. Mekawy, H. Nguyen, W. Warkocki and M. Ohnuma, Mesoporous Silica Nanotubes Hybrid Membranes for Functional Nanofiltration, *Nanotechnology*, 2010, **21**, 375603.
62 S. A. El-Safty; M. K. Shenashen; A. Shahat. Separation of Macromolecules by Hexagonal Mesoporous Membrane Filters, in *Recent Researches in Modern Medicine*, 2011, pp. 324–329.
63 S. El-Safty, A. Shahat and H. Nguyen, Nano-model Membrane Filters for the Well-controlled Separation of Biomolecules, *Colloids Surf. A, Physicochem. Eng. Aspects*, 2011, **377**, 44–53.
64 M. M. Mekawy, A. Yamaguchi, S. A. El-Safty, T. Itoh and N. Teramae, Mesoporous Silica Hybrid Membranes for Precise Size-exclusive Separation of Silver Nanoparticles, *J. Colloid Interface Sci.*, 2011, **355**, 348–358.
65 T. Itoh, T. Shimomura, Y. Hasegawa, J. Mizuguchi, T. Hanaoka, A. Hayashi, A. Yamaguchi, N. Teramae, M. Ono and F. Mizukami, Assembly of an Artificial Biomembrane by Encapsulation of an Enzyme, Formaldehyde Dehydrogenase, into the Nanoporous-walled Silica Nanotube–Inorganic Composite Membrane, *J. Mater. Chem.*, 2011, **21**, 251–256.
66 S. El-Safty and M. A. Shenashen, Size-selective Separations of Biological Macromolecules on Mesocylinder Silica Arrays, *Anal. Chim. Acta*, 2011, **694**, 151–161.
67 S. El-Safty, A. Shahat, M. R. Awual and M. Mekawy, Large Three-dimensional Mesocage Pores Tailoring Silica Nanotubes as Membrane Filters: Nanofiltration and Permeation Flux of Proteins, *J. Mater. Chem.*, 2011, **21**, 5593–5603.
68 Y. Yamaguchi, A. Sugiyama, M. Sawada, M. Komatsu, A. Takai, C. Urata, N. Hirota, Y. Sakka and K. Kuroda, Magnetically Induced Orientation of Mesochannels Inside Porous Anodic Alumina Membranes Under Ultra High Magnetic Field of 30 T: Confirmation by TEM, *J. Ceram. Soc. Jpn.*, 2008, **116**, 1244–1248.
69 L. Guo, Y. Fan and N. Teramae, Vapor Phase Synthesis of Mesoporous Silica Rods Within the Pores of Alumina Membranes, *New J. Chem.*, 2012, **36**, 1301–1303.
70 J. J. Hill, S. P. Cotton and K. J. Ziegler, Alignment and Morphology Control of Ordered Mesoporous Silicas in Anodic Aluminum Oxide Channels by Electrophoretic Deposition, *Chem. Mater.*, 2009, **21**, 1841–1846.
71 X. Ren and Z. Lun, Mesoporous Silica Nanowires Synthesized by Electrodeposition in AAO, *Mater. Lett.*, 2012, **68**, 228–229.
72 L. Guo, Y. Fan, H. Arafune and N. Teramae, Hierarchically Structured Periodic Mesoporous Silica by Vapor Phase Synthesis, *Microporous Mesoporous Mater.*, 2012, **162**, 122–130.
73 S. A. El-Safty, M. Mekawy, A. Yamaguchi, A. Shahat, K. Ogawa and N. Teramae, Organic–Inorganic Mesoporous Silica Nanostrands for Ultrafine Filtration of Spherical Nanoparticles, *Chem. Commun.*, 2010, **46**, 3917–3919.

